

Revision 2

1  
2 Pauloabibite, trigonal  $\text{NaNbO}_3$ , isostructural with  
3 ilmenite, from the Jacupiranga carbonatite, Cajati, São  
4 Paulo, Brazil.

5  
6 Luiz A.D. Menezes Filho<sup>1\*</sup>,

7 Daniel Atencio<sup>2</sup>,

8 Marcelo B. Andrade<sup>3</sup>,

9 Robert T. Downs<sup>3</sup>,

10 Mário L.S.C. Chaves<sup>1</sup>,

11 Antônio W. Romano<sup>1</sup>,

12 Ricardo Scholz<sup>4</sup>

13 Aba I. C. Persiano<sup>5</sup>

14 <sup>1</sup>Instituto de Geociências, Universidade Federal de Minas Gerais, Avenida Antônio Carlos, 6627,  
15 31270-901, Belo Horizonte, Minas Gerais, Brazil

16 <sup>2</sup>Instituto de Geociências, Universidade de São Paulo, Rua do Lago 562, 05508-080, São Paulo,  
17 SP, Brazil

18 <sup>3</sup>Instituto de Física de São Carlos, Universidade de São Paulo, Caixa Postal 369, 13560-970, São  
19 Carlos, SP, Brazil

20 <sup>4</sup>Departamento de Geologia da Escola de Minas da Universidade Federal de Ouro Preto, Campus  
21 Morro do Cruzeiro, Ouro Preto, 35400-000, Minas Gerais, Brazil

22 <sup>5</sup>Departamento de Física do Instituto de Ciências Exatas da Universidade Federal de Minas  
23 Gerais, Avenida Antônio Carlos, 6627, 31279-901, Belo Horizonte, Minas Gerais, Brazil

24 \*E-mail: [lmenezesminerals@gmail.com](mailto:lmenezesminerals@gmail.com)

25

26  
27 ABSTRACT  
28

29 Pauloabibite (IMA 2012-090), trigonal  $\text{NaNbO}_3$ , occurs in the Jacupiranga carbonatite, in  
30 Cajati County, São Paulo State, Brazil, associated with dolomite, calcite, magnetite, phlogopite,  
31 pyrite, pyrrhotite, ancylite-(Ce), tochilinite, fluorapatite, “pyrochlore”, vigezzite, and strontianite.  
32 Pauloabibite occurs as encrustations of platy crystals, up to 2 mm in size, partially intergrown  
33 with an unidentified Ca-Nb-oxide, embedded in dolomite crystals, which in this zone of the mine  
34 can reach centimeter sizes. Cleavage is perfect on  $\{001\}$ . Pauloabibite is transparent and displays  
35 a sub-adamantine luster; it is pinkish brown and the streak is white. The calculated density is  
36  $4.246 \text{ g/cm}^3$ . The mineral is uniaxial;  $n(\text{mean})_{\text{calc.}}$  is 2.078. Chemical composition ( $n=17$ , WDS,  
37 wt.%) is:  $\text{Na}_2\text{O}$  16.36,  $\text{MgO}$  0.04,  $\text{CaO}$  1.36,  $\text{MnO}$  0.82,  $\text{FeO}$  0.11,  $\text{SrO}$  0.02,  $\text{BaO}$  0.16,  $\text{SiO}_2$   
38 0.03,  $\text{TiO}_2$  0.86,  $\text{Nb}_2\text{O}_5$  78.66,  $\text{Ta}_2\text{O}_5$  0.34, total 98.76. The empirical formula is  
39  $(\text{Na}_{0.88}\text{Ca}_{0.04}\text{Mn}^{2+}_{0.02})_{\Sigma 0.94}(\text{Nb}_{0.98}\text{Ti}_{0.02})_{\Sigma 1.00}\text{O}_3$ . X-ray powder-diffraction lines (calculated pattern)  
40 [ $d$  in  $\text{Å}(I)(hkl)$ ] are: 5.2066(100)(003), 4.4257(82)(101), 3.9730(45)(012), 2.9809(54)(104),  
41 2.3718(88)(2-13), 1.9865(28)(024), 1.8620(53)(2-16), and 1.5383 (30) (300). It is trigonal, space  
42 group:  $R\bar{3}$ ,  $a = 5.3287(5)$ ,  $c = 15.6197(17) \text{ Å}$ ,  $V = 384.10(7) \text{ Å}^3$ ,  $Z = 6$ . The crystal structure was  
43 solved ( $R_1 = 0.0285$ ,  $wR_2 = 0.0636$  for 309 observed reflections). Pauloabibite is isostructural  
44 with ilmenite and is polymorphic with isolueshite (cubic) and lueshite (orthorhombic). The name  
45 is in honour of Professor Paulo Abib Andery (1922-1976).

46  
47 **Keywords:** pauloabibite, new mineral, carbonatite, ilmenite structure, crystal structure, chemical  
48 composition, Jacupiranga mine, Cajati, Brazil

## INTRODUCTION

52

53

54 Pauloabibite (IMA 2012-090), trigonal  $\text{NaNbO}_3$ , is polymorphic with isolueshite (cubic)  
55 and lueshite (orthorhombic) (Table 1). Natroniobite, a poorly described mineral (Bulakh et al.  
56 1960), may be a monoclinic polymorph of  $\text{NaNbO}_3$ , or a mineral with formula  $\text{NaNb}_2\text{O}_5(\text{OH})$ ,  
57 related to fersmite (Chakhmouradian et al. 1997, Chakhmouradian and Mitchell 1998).  
58 Chakhmouradian and Mitchell (1998) investigated a museum specimen labeled “natroniobite”  
59 (not the type specimen) and concluded that it is a “complex aggregate of lueshite and its  
60 replacement products, set in a matrix of dolomite and fluorapatite”. Monoclinic synthetic  
61 compounds with formula  $\text{NaNbO}_3$  are known (e.g. Solov’ev et al. 1961; Johnston et al. 2010), but  
62 the X-ray diffraction pattern of natroniobite does not match those of these other compounds.

63 Pauloabibite is trigonal, isostructural with ilmenite and other  $R\text{-}3$  oxides which display a  
64 crystal structure formed by the hexagonal close packing of oxygen atoms, with two-thirds of the  
65 octahedral interstices occupied by two unique sites of di- and tetravalent or uni- and pentavalent  
66 cations. In corundum and other  $R\text{-}3c$  oxides, two-thirds of the octahedral interstices are occupied  
67 by trivalent cations in one unique site. Data for these minerals are included in Table 2.

68 The synthetic analogue of pauloabibite has been studied by several research groups. It  
69 was reported by Kinomura et al. (1984) and Kumata et al. (1990) from a two-step synthesis  
70 method, involving the preparation of  $\text{Na}_8\text{Nb}_6\text{O}_{19}\cdot 13\text{H}_2\text{O}$  followed by hydrothermal reaction with  
71 NaOH in a silver-lined vessel at 250°C. It was also prepared directly in one step under mild  
72 hydrothermal conditions by lowering pH and using close-to-stoichiometric amounts of reagents  
73 at 240°C (Modeshia et al. 2009; Johnston et al. 2011). The equivalent to lueshite (space group  
74  $Pbnm$ ) was not yet synthesized, but phase transitions in natural lueshite were observed in the  
75 sequence:  $Cmcm$  at 575°C,  $P4/mbm$  at 625°C, and  $Pm\text{-}3m$ , equivalent to isolueshite, at 650 °C  
76 (Mitchell et al. 2014).

77 The name is in honor of Professor Paulo Abib Andery (1922-1976), Department of  
78 Mining Engineering at the Polytechnic School, Universidade de São Paulo, who developed a  
79 flotation process for Serrana SA Mining, resulting in an apatite concentrate that is used as raw  
80 material for the production of phosphoric acid and a calcite tailing that is used for the  
81 manufacture of cement. He founded the mining research facility known as Paulo Abib

82 Engenharia in the early 1970s, a pioneering institution in developing ore dressing technology in  
83 Brazil.

84 Type material (specimen number DR740) is deposited in the Museu de Geociências,  
85 Instituto de Geociências, Universidade de São Paulo, Rua do Lago, 562, 05508-080 - São Paulo,  
86 SP, Brazil.

87

88

## OCCURRENCE

89

90 The mineral occurs in the Jacupiranga carbonatite (24°43'47"S, 48°06'37"W), Cajati  
91 County, São Paulo State, Brazil (Menezes and Martins 1984). This property is located near the  
92 Southern border of the Jacupiranga Igneous Complex, an alkaline intrusion that was formed in a  
93 continental-rift environment in the Early Cretaceous, with the age estimated at 130 m.a. (Roden  
94 et al. 1985), that outcrops in an area of 65 km<sup>2</sup>, and constitutes dunites and peridotites in its  
95 Northern part and jacupirangite, ijolite and nepheline syenites in the Southern; the carbonatite  
96 plug is totally intruded into jacupirangite.

97 The carbonatite has been extensively mined since the late 1960's for the production of  
98 apatite and calcite; the average composition is 74% carbonates (calcite, dolomite and ankerite);  
99 12% fluorapatite, 8% magnetite 2% phlogopite, 2% olivine, 1% sulphides and 1% of other  
100 accessory minerals (Alves 2008). It formed as a series of 5 successive intrusions. The oldest  
101 carbonatite, C1, was probably derived from a magma somewhat different chemically from those  
102 producing carbonatites C2 through C5. The precipitation of carbonatite C2 probably went to  
103 completion independently of C3 through C5, whereas carbonatites C3 through C5 probably were  
104 precipitated from successive batches of magma representing a continuum in time and magmatic  
105 evolution (Gaspar and Willye 1983). Pauloabite was found in the transition between the  
106 intrusions C2 and C3, where the carbonatite is coarser and a pyrochlore-group mineral is present  
107 as an accessory mineral; in this zone two other unique species were found: quintinite (Chao and  
108 Gault 1997) and menezesite (Atencio et al. 2008). Associated minerals are dolomite, calcite,  
109 magnetite, phlogopite, pyrite, pyrrhotite, ancylite-(Ce), tochilinite, fluorapatite, "pyrochlore",  
110 vigezzite, and strontianite. Pauloabite occurs embedded in dolomite crystals, which in this zone  
111 of the mine can reach centimetre sizes.

112

113

114

## HABIT AND PHYSICAL PROPERTIES

115

116 The mineral occurs as encrustations of platy crystals to 2 mm in size in dolomite. Crystals  
117 are partially intergrown with a still unidentified Ca-Nb oxide (Figures 1 and 2). Cleavage is  
118 perfect on {001} and parting was not observed. Pauloabibite is transparent and displays a sub-  
119 adamantine lustre; it is pinkish brown and the streak is white. It is non-fluorescent under short  
120 (254 nm) or long wavelength (366 nm) ultraviolet radiation. The Mohs hardness was not  
121 measured due to the small crystal size. Fracture is irregular and the grains are fragile due to  
122 perfect cleavage. Density was not measured due to the paucity of material but the calculated  
123 density is 4.246 g/cm<sup>3</sup> (based on empirical formula). Optically the mineral is uniaxial;  
124  $n(\text{mean})_{\text{calc.}}$  is 2.078 using the Gladstone-Dale relationship (Mandarino 1979), higher than that of  
125 available immersion liquids.

126

127

128

## MINERAL CHEMISTRY

129

130 Pauloabibite crystals were embedded in epoxy resin and polished. Chemical analyses (17)  
131 were completed with a JEOL JXA-8900 electron microprobe (WDS mode, 15 kV, 20 nA, ~1  $\mu\text{m}$   
132 beam diameter). Analytical results are represented in Table 3. No elements with  $Z > 8$  other than  
133 those reported were indicated by EDS. The empirical formula [based on 3 O *apfu*] is:  
134  $(\text{Na}_{0.88}\text{Ca}_{0.04}\text{Mn}^{2+}_{0.02})_{\Sigma 0.94}(\text{Nb}_{0.98}\text{Ti}_{0.02})_{\Sigma 1.00}\text{O}_3$ . The ideal formula  $\text{NaNbO}_3$  yields the following  
135 wt% oxide values:  $\text{Na}_2\text{O} = 18.91$ ,  $\text{Nb}_2\text{O}_5 = 81.09$ , Total 100.00.

136

137

138

## CRYSTAL STRUCTURE DETERMINATION

139

140 Very strong preferential orientation effects were observed in the powder X-ray diffraction  
141 data (XRD) due to the perfect {001} cleavage. The observed pattern probably would be of little  
142 value due to a huge difference between calculated and observed intensities of reflections. We

143 present only the model X-ray powder diffraction pattern (Table 4) calculated from the determined  
144 structure model using the XPOW program by Downs et al. (1993).

145 A single crystal ( $0.09 \times 0.07 \times 0.06$  mm) was selected for intensity measurements on a  
146 Bruker X8 APEX2 CCD diffractometer using graphite-monochromatized  $\text{MoK}\alpha$  ( $\lambda = 0.71073$  Å)  
147 radiation. Data were collected to a  $2\theta$  value of  $65^\circ$  and the X-ray absorption correction was  
148 calculated by the MULTI-SCAN method using the Bruker program SADABS (Sheldrick 1996).  
149 The crystal structure was solved using direct methods and refined using SHELX97 (Sheldrick  
150 2008). Due to the measured major element chemistry, for simplicity, the structure was refined  
151 using the ideal formula,  $\text{NaNbO}_3$ , as the overall effects of minor elements (Ca, Mn and Ti) on the  
152 final structure results are negligible. Details about the data collection and structure refinement are  
153 summarized in Table 5. The final atom coordinates and anisotropic thermal displacement  
154 parameters are listed in Table 6. Selected bond distances, angles and bond valence calculations  
155 using the parameters given by Brese and O'Keeffe (1991) are in Table 7. Structure factors for  
156 pauloabibite and the CIF file are provided as deposited material<sup>1</sup>.

157 <sup>1</sup> Deposit item AM-14-XXX, CIF and structure factors. Deposit items are available two  
158 ways: For a paper copy, contact the Business Office of the Mineralogical Society of America (see  
159 inside front cover of recent issue) for price information. For an electronic copy visit the MSA  
160 web site at <http://www.minsocam.org>, go to the *American Mineralogist* Contents, find the table  
161 of contents for the specific volume/issue wanted, and then click on the deposit link there.

162 Pauloabibite ( $\text{NaNbO}_3$ ) is isostructural with ilmenite. It has a layered structure, in which  
163  $\text{NaO}_6$  and  $\text{NbO}_6$  distorted octahedra share edges to form fully ordered Na and Nb layers that are  
164 stacked alternating along the *c* axis (Figure 3). The mean Nb–O (2.004 Å) and Na–O (2.412 Å)  
165 distances are in agreement with those determined by Modeshia et al. (2009) in their work on  
166 synthetic  $\text{NaNbO}_3$  isomorphic with ilmenite: Nb–O (2.01 Å) and Na–O (2.41 Å). Isolueshite, the  
167 cubic polymorph, and lueshite, the orthorhombic polymorph, display modified perovskite  
168 structures, with distorted  $\text{NaO}_{12}$  cuboctahedral polyhedra and  $\text{NbO}_6$  octahedra (Krivovichev et al.  
169 2000; Mitchell et al. 2014).

170

171

172

## IMPLICATIONS

173

174 Much work has been carried out on the synthesis of alkaline niobates because of their  
175 excellent nonlinear optical, ferroelectric, piezoelectric, electro-optic, ionic conductive,  
176 pyroelectric, photorefractive, selective ion exchange, and photocatalytic properties. For example,  
177 lead-free potassium and sodium niobates are potential substitutes for lead zirconium titanate  
178 (PZT,  $\text{PbZr}_x\text{Ti}_{1-x}\text{O}_3$ , one of the world's most widely used high-performance piezoelectric  
179 ceramics). The high lead content in PZT introduces serious concerns about environment pollution  
180 during the fabrication, use and disposal of the materials, and therefore, because increasing  
181 attention has been paid to environmental issues nowadays, potential substitutes are urgently being  
182 examined (Wu et al. 2010).

183  $\text{NaNbO}_3$  is known to exhibit a rich polymorphism based on the perovskite structure, with  
184 a number of displacive transition occurring over a range of temperatures, which may also be  
185 sensitive to both pressure and crystallite size. Doped forms of the material are currently the focus  
186 of much attention because of their piezoelectric properties (Modeshia et al. 2009).

187

188

#### 189 ACKNOWLEDGEMENTS

190

191 We acknowledge the Brazilian agencies FAPESP (processes 2008/04984-7, 2011/22407-  
192 0), CNPq, and Finep for financial support, and all members of the IMA Commission on New  
193 Minerals, Nomenclature and Classification, the Editor Fernando Colombo, and the reviewers  
194 Stuart Mills and Cristian Biagioni for their helpful suggestions and comments.

195

196

#### 197 REFERENCES

198

199 Alves, P.R. (2008) The carbonatite-hosted apatite deposit of Jacupiranga, SE Brazil: styles of  
200 mineralization, ore characterization and association with mineral processing. Master Thesis  
201 – Missouri University of Science and Technology.

202 Atencio, D., Coutinho, J.M.V., Doriguetto, A.C., Mascarenhas, Y.P., Ellena, J.A., and Ferrari,  
203 V.C. (2008) Menezesite, the first natural heteropolyniobate, from Cajati, São Paulo, Brazil:  
204 Description and crystal structure. *American Mineralogist*, 93, 81-87.

- 205 Birch, W.D., Burke, E.A.J., Wall, V.J., and Etheridge, M.A. (1988) Ecandrewsite, the zinc  
206 analogue of ilmenite, from Little Broken Hill, New South Wales, Australia, and the San  
207 Valentin Mine, Sierra de Cartagena, Spain. *Mineralogical Magazine*, 52, 237-240.
- 208 Brese, N.E. and O'Keeffe, M. (1991) Bond-valence parameters for solids. *Acta*  
209 *Crystallographica*, B47, 192-197.
- 210 Bulakh, A.G., Kukharenko, A.A., Knipovich, Yu.N., Kondrat'eva, V.V., Baklanova, K.A., and  
211 Baranova, E.N. (1960) Some new minerals in carbonatites of the Kola Peninsula. *Mater.*  
212 *God. Sessii Uchenogo Sov. VSEGEI (Mat. Ann. Sci. Coincil Meeting)*, 1959, 114-116 (in  
213 Russian).
- 214 Chakhmouradian, A.R. and Mitchell, R.H. (1998) Lueshite, pyrochlore and monazite-(Ce) from  
215 apatite-dolomite carbonatite, Lesnaya Varaka complex, Kola Peninsula, Russia.  
216 *Mineralogical Magazine*, 62, 769-782.
- 217 Chakhmouradian, A.R., Yakovenchuk, V.N., Mitchell, R.H., and Bogdanova, A.N. (1997)  
218 Isolueshite, a new mineral of the perovskite group from the Khibina alkaline complex.  
219 *European Journal of Mineralogy*, 9, 483-490.
- 220 Chao, G.Y. and Gault, R.A. (1997) Quintinite-2H, quintinite-3T, charmarite-2H, charmarite-3T  
221 and caresite-3T, a new group of carbonate minerals related to the hydrotalcite-manasseite  
222 group. *Canadian Mineralogist*, 35, 1541-1549.
- 223 Downs, R.T., Bartelmehs, K.L., Gibbs, G.V., and Boisen, M.B. (1993) Interactive software for  
224 calculating and displaying X-ray or neutron powder diffractometer patterns of crystalline  
225 materials. *American Mineralogist*, 78, 1104-1107.
- 226 Gaspar, J.C. and Willye, P.J. (1983) Magnetite in carbonatites from the Jacupiranga Complex,  
227 Brazil. *American Mineralogist*, 68, 195-213.
- 228 Johnston, K.E., Griffin, J.M., Walton, R.I., Dawson, D.M., Lightfoot, P., and Ashbrook, S.E.  
229 (2011) <sup>93</sup>Nb NMR and DFT investigation of the polymorphs of NaNbO<sub>3</sub>. *Physical*  
230 *Chemistry and Chemical Physics*, 13, 7565-7576.
- 231 Johnston, K.E., Tang, C.C., Parker, J.E., Knight, K.S., Lightfoot, P., and Ashbrook, S.E. (2010)  
232 The polar phase of NaNbO<sub>3</sub>: a combined study by powder diffraction, solid-state NMR, and  
233 first-principles calculations. *Journal of the American Chemical Society*, 132(25), 8732-  
234 8746.



- 235 Kidoh, K., Tanaka, K., Marumo, F., and Takei, H. (1984) Electron density distribution in  
236 ilmenite-type crystals. II. Manganese (II) titanium (IV) trioxide. *Acta Crystallographica*,  
237 B40, 329-332.
- 238 Kinomura, N., Kumata, N., and Muto, F. (1984) A new allotropic form with ilmenite-type  
239 structure of  $\text{NaNbO}_3$ . *Materials Research Bulletin*, 19, 299-304.
- 240 Kirfel, A. and Eichhorn, K. (1990) Accurate structure analysis with synchrotron radiation. The  
241 electron density in  $\text{Al}_2\text{O}_3$  and  $\text{Cu}_2\text{O}$ . *Acta Crystallographica*, A46, 271-284
- 242 Krivovichev, S.V., Chakhmouradian, A.R., Mitchell, R.H., Filatov, S.K., and Chukanov, N.V.  
243 (2000) Crystal structure of isolueshite and its synthetic compositional analogue. *European*  
244 *Journal of Mineralogy*, 12, 597-607
- 245 Kukhareenko, A.A., Orlova, M.P., Bulakh, A.G., Bagdasarov, E.A., Rimskaya-Korsakova, O.M.,  
246 Nefedov, E.I., Il'inskii, G.A., Sergeev, A.S., and Abakumova, N.B. (1965) The Caledonian  
247 complex of ultrabasic alkaline rocks and carbonatites of the Kola Peninsula and Northern  
248 Karelia. Nedra Press, Leningrad (in Russian), 772 pp.
- 249 Kumata, N., Kinomura, N., and Muto, F. (1990) Crystal structure of ilmenite-type  $\text{LiNbO}_3$  and  
250  $\text{NaNbO}_3$ . *Journal of the Ceramic Society of Japan*, 98, 384-388.
- 251 Liferovich, R.P. and Mitchell, R.H. (2006) The pyrophanite–geikielite solid-solution series:  
252 crystal structures of the  $\text{Mn}_{1-x}\text{Mg}_x\text{TiO}_3$  series ( $0 < x < 0.7$ ). *Canadian Mineralogist*, 44,  
253 1099-1107.
- 254 Long, J.V.P., Vuorelainen, Y., and Kouvo, O. (1963) Karelianite, a new vanadium mineral.  
255 *American Mineralogist*, 48, 33–41.
- 256 Ma, Chi and Rossman, G.R. (2009) Tistarite,  $\text{Ti}_2\text{O}_3$ , a new refractory mineral from the Allende  
257 meteorite. *American Mineralogist*, 94, 841-844.
- 258 Mandarino, J.A. (1979) The Gladstone-Dale relationship. III. Some general applications.  
259 *Canadian Mineralogist*, 19, 441-450.
- 260 Maslen, E.N., Streltsov, V.A., Streltsova, N.R., and Ishizawa, N. (1994) Synchrotron X-ray study  
261 of the electron density in  $\alpha\text{-Fe}_2\text{O}_3$ . *Acta Crystallographica*, B50, 435-441.
- 262 Menezes, L.A.D., Fo. and Martins, J.M. (1984) The Jacupiranga mine, São Paulo, Brazil.  
263 *Mineralogical Record*, 15, 261-270.

- 264 Mitchell, R.H., Burns, P.C., Knight, K.S., Howard, C.J., and Chakhmouradian, A.R. (2014)  
265 Observations on the crystal structures of lueshite. *Physics and Chemistry of Minerals* (in  
266 press).
- 267 Modeshia, D.R., Darton, R.J., Ashbrook, S.E., and Walton, R.I. (2009) Control of polymorphism  
268 in  $\text{NaNbO}_3$  by hydrothermal synthesis. *Chemical Communications*, 68-70.
- 269 Moore, P.B. (1968) Substitutions of the type  $(\text{Sb}^{5+}_{0.5}\text{Fe}^{3+}_{0.5}) \leftrightarrow (\text{Ti}^{4+})$ : the crystal structure of  
270 melanostibite. *American Mineralogist*, 53, 1104-1109.
- 271 Newnham, R.E. and de Haan, Y.M. (1962) Refinement of the  $\alpha$   $\text{Al}_2\text{O}_3$ ,  $\text{Ti}_2\text{O}_3$ ,  $\text{V}_2\text{O}_3$  and  $\text{Cr}_2\text{O}_3$   
272 structures. *Zeitschrift für Kristallographie*, 117, 235-237.
- 273 Olmi, F. and Sabelli, C. (1994) Brizziite,  $\text{NaSbO}_3$ , a new mineral from the Cetine mine (Tuscany,  
274 Italy): description and crystal structure. *European Journal of Mineralogy*, 6, 667-672.
- 275 Roden, M.F., Murthy, V.R., and Gaspar, J.C. (1985) Sr and Nd isotropic composition of the  
276 Jacupiranga carbonatite. *Journal of Geology*, 93(2), 212-220.
- 277 Safiannikoff, A. (1959) Un nouveau mineral de niobium, Académie Royal des Sciences d'Outre-  
278 Mer, *Bulletin dès Séances*, 5, 1251-1255.
- 279 Sheldrick, G.M. (1996) SADABS, Absorption Correction Program. University of Göttingen,  
280 Germany.
- 281 Sheldrick, G.M. (2008) A short history of SHELX. *Acta Crystallographica*, A64, 112–122.
- 282 Solov'ev, S.P., Venevtsev, Y.N., and Zhanov, G. S. (1961) An x-ray study of phase transitions in  
283  $\text{NaNbO}_3$ . *Soviet Physics Crystallography* 6, 171-175.
- 284 Tomioka, N. and Fujino, K. (1999) Akimotoite,  $(\text{Mg,Fe})\text{SiO}_3$ , a new silicate mineral of the  
285 ilmenite group in the Tenham chondrite. *American Mineralogist*, 84, 267-271
- 286 Waerenborgh, J.C., Figueiras, J., Mateus, A., and Gonçalves, M. (2002) Nature and mechanism  
287 of ilmenite alteration: a Mössbauer and X-ray diffraction study of oxidized ilmenite from  
288 the Beja-Acebuches Ophiolite Complex (SE Portugal). *Mineralogical Magazine*, 66, 421-  
289 430.
- 290 Wu, S.Y., Zhang, W., and Chen, X.M. (2010) Formation mechanism of  $\text{NaNbO}_3$  powders during  
291 hydrothermal synthesis. *Journal of Materials Science: Materials in Electronics*, 21, 450–  
292 455.
- 293

294

295 Table 1. Comparative data for NaNbO<sub>3</sub> polymorphs.

296

Mineral	pauloabibite	isolueshite	lueshite	natroniobite
Formula	NaNbO <sub>3</sub>	NaNbO <sub>3</sub>	NaNbO <sub>3</sub>	NaNbO <sub>3</sub> (?)
Crystal system	trigonal	cubic	orthorhombic	monoclinic (?)
Space group	$R\bar{3}$	$Pm\bar{3}m$	$Pbnm$	n.d.
<i>a</i> (Å)	5.3287(5)	3.909(1)	5.5269(10)	
<i>b</i> (Å)			5.5269(10)	
<i>c</i> (Å)	15.6197(17)		7.8180(10)	
<i>V</i> (Å <sup>3</sup> )	384.10(7)	59.73(3)	238.81	
<i>Z</i>	6	1	4	
Strongest lines in XRPD pattern;	5.2066 (100)	3.915 (30)	3.91 (100)	4.81 (70)
<i>d</i> in Å ( <i>I</i> <sub>rel</sub> )	4.4257 (82)	2.765 (100)	2.77 (70)	3.77 (20)
	3.9730 (45)	1.953 (50)	1.96 (70)	3.05 (100)
	2.9809 (54)	1.747 (10)	1.748 (20)	2.97 (20)
	2.3718 (88)	1.594 (30)	1.60 (30)	2.77 (20)
	1.9865 (28)	1.380 (20)	1.382 (10)	2.68 (50)
	1.8620 (53)	1.234 (10)	1.302 (10)	1.72 (30)
	1.5383 (30)	1.042 (10)	1.234 (10)	1.61 (30)
Calculated density (g cm <sup>-3</sup> )	4.246	4.57	4.559	4.4 (meas.)
Color	pinkish brown	brownish-black	black	yellowish, brownish, blackish
Luster	vitreous	adamantine		
Optical class	Uniaxial	Isotropic	Biaxial (-)	Biaxial (-)
<i>n</i>	2.078 (mean, calc.)	2.200	2.29-2.30 (mean)	
<i>α</i>				2.10-2.13
<i>β</i>				2.19-2.21
<i>γ</i>				2.21-2.24
2 <i>V</i> (meas.) (°)			46	10-30
Reference	this proposal, calculated XRPD pattern	Chakhmouradian et al. (1997); Krivovichev et al. (2000)	Safiannikoff (1959); Mitchell et al. (2014)	Kukhareenko et al. (1965)

297

298

299 Table 2. Chemical composition and crystallographic data for pauloabibite and related minerals.

mineral	formula	Space group	a	c	reference
corundum	Al <sub>2</sub> O <sub>3</sub>	<i>R-3c</i>	4.7570(6)	12.9877(35)	Kirfel and Einchhorn (1990)
akimotoite	MgSiO <sub>3</sub>	<i>R-3</i>	4.78(5)	13.6(1)	Tomioka and Fujino (1999)
eskolaite	Cr <sub>2</sub> O <sub>3</sub>	<i>R-3c</i>	4.9607(10)	13.599(5)	Newnham and de Haan (1962)
karelianite	V <sub>2</sub> O <sub>3</sub>	<i>R-3c</i>	4.99	13.98	Long et al. (1963)
hematite	Fe <sup>3+</sup> <sub>2</sub> O <sub>3</sub>	<i>R-3c</i>	5.0355(5)	13.7471(7)	Maslen et al. (1994)
geikielite	MgTi <sup>4+</sup> O <sub>3</sub>	<i>R-3</i>	5.0567(0)	13.9034(2)	Liferovich and Mitchell (2006)
ilmenite	Fe <sup>2+</sup> Ti <sup>4+</sup> O <sub>3</sub>	<i>R-3</i>	5.070(1)	14.064(3)	Waerenborgh et al. (2002)
ecandrewsite	ZnTi <sup>4+</sup> O <sub>3</sub>	<i>R-3</i>	5.090(1)	14.036(2)	Birch et al. (1988)
pyrophanite	Mn <sup>2+</sup> Ti <sup>4+</sup> O <sub>3</sub>	<i>R-3</i>	5.13948(7)	14.2829(4)	Kidoh et al. (1984)
tistarite	Ti <sup>3+</sup> <sub>2</sub> O <sub>3</sub>	<i>R-3c</i>	5.158	13.611	Ma and Rossman (2009)
melanostibite	Mn <sup>2+</sup> (Sb <sup>5+</sup> ,Fe <sup>3+</sup> )O <sub>3</sub>	<i>R-3</i>	5.226(5)	14.325(5)	Moore (1968)
brizziite	NaSb <sup>5+</sup> O <sub>3</sub>	<i>R-3</i>	5.301(1)	15.932(4)	Olmi and Sabelli. (1994)
pauloabibite	NaNbO <sub>3</sub>	<i>R-3</i>	5.3287(5)	15.6197(17)	This paper

300

301

302

303

Table 3. Analytical data for pauloabibite (mean of 17 point analyses).

Constituent	wt%	Range	Standard deviation	Probe standard
Na <sub>2</sub> O	16.36	13.39-19.40	1.60	jadeite
MgO	0.04	0.00-0.19	0.06	dolomite
CaO	1.36	0.16-5.38	1.52	anorthite
MnO	0.82	0.06-1.73	0.46	rhodonite
FeO	0.11	0.00-0.65	0.16	siderite
SrO	0.02	0.00-0.22	0.06	celestine
BaO	0.16	0.00-0.83	0.22	barite
SiO <sub>2</sub>	0.03	0.00-0.11	0.03	quartz
TiO <sub>2</sub>	0.86	0.06-1.98	0.74	rutile
Nb <sub>2</sub> O <sub>5</sub>	78.66	72.10-84.32	3.84	Nb metal
Ta <sub>2</sub> O <sub>5</sub>	0.34	0.00-0.91	0.29	Ta metal
Total	98.76			

304

305

Table 4. X-ray powder diffraction data for pauloabibite.

$d_{calc.}(\text{\AA})$	$I_{calc.}$	$h$	$k$	$l$
5.2066	100	0	0	3
4.4257	82	1	0	1
3.9730	45	0	1	2
2.9809	54	1	0	4
2.6644	13	1	1	0
2.6033	3	0	0	6
2.3718	88	2	-1	3
2.3718	9	1	1	3
2.0089	4	1	0	7
1.9865	28	0	2	4
1.8620	53	2	-1	6
1.8620	16	1	1	6
1.7981	8	0	1	8
1.7335	8	3	-1	1
1.7023	5	-1	3	2
1.6040	15	0	2	7
1.5926	3	2	1	4
1.5926	21	3	-1	4
1.5383	30	3	0	0
1.4795	9	1	0	10
1.4752	5	0	3	3
1.4752	6	3	0	3
1.4542	14	1	1	9
1.3742	3	2	1	7
1.3322	4	2	2	0
1.2935	6	0	2	10
1.2906	6	2	2	3
1.2756	5	1	3	1

1.2631	5	3	1	2
1.2162	7	1	3	4
1.1859	5	2	2	6
1.1636	6	2	1	10

308

309 Table 5. Summary of crystal data and refinement results for pauloabibite

310	Ideal chemical formula	NaNbO <sub>3</sub>
311	Crystal symmetry	trigonal
312	Space group	<i>R</i> -3 (no. 148)
313	<i>a</i> (Å)	5.3287 (5)
314	<i>c</i> (Å)	15.6197 (17)
315	<i>V</i> (Å <sup>3</sup> )	384.10(7)
316	<i>Z</i>	6
317	$\rho_{\text{cal}}$ (g/cm <sup>3</sup> )	4.251
318	$\lambda$ (Å, MoK $\alpha$ )	0.71073
319	$\mu$ (mm <sup>-1</sup> )	4.60
320	2 $\theta$ range for data collection	$\leq 65$
321	No. of reflections collected	1155
322	No. of independent reflections	309
323	No. of reflections with $I > 2\sigma(I)$	275
324	No. of parameters refined	18
325	<i>R</i> (int)	0.044
326	Final <i>R</i> <sub>1</sub> , <i>wR</i> <sub>2</sub> factors [ $I > 2\sigma(I)$ ]	0.029, 0.064
327	Goodness-of-fit	1.06



328

Table 6. Atom coordinates and displacement parameters ( $\text{\AA}^2$ ) for pauloabibite.

	$x/a$	$y/b$	$z/c$	$U_{\text{eq}}$	$U_{11}$	$U_{22}$	$U_{33}$	$U_{23}$	$U_{13}$	$U_{12}$
Na	0	0	0.35846(17)	0.0136(5)	0.0147(8)	0.0147(8)	0.0113(12)	0.0000(0)	0.0000(0)	0.0073(4)
Nb	0	0	0.14867(3)	0.0068(2)	0.0064(2)	0.0064(2)	0.0075(3)	0.0000(0)	0.0000(0)	0.0032(1)
O	0.3239(5)	0.0532(6)	0.23828(16)	0.0095(5)	0.0089(12)	0.0099(12)	0.0098(11)	0.0014(9)	-0.0002(9)	0.0047(10)

329

330 Table 7. Selected bond lengths, angles, and bond valence (BV) calculations in the refined pauloabibite structure.

331

Bond	Bond length	BV(v.u)	$\Sigma$
Nb-O	1.881(3)	1.084 (x3)	3.252
Nb-O	2.182(2)	0.481 (x3)	1.443
			4.695
Na-O	2.354(3)	0.226 (x3)	0.678
Na-O	2.469(3)	0.165 (x3)	0.495
			1.173
	Angles		
O-Nb-O	77.65 (11), 81.44 (10), 99.23 (14), 101.70 (9)		
O-Na-O	68.45 (11), 90.09 (12), 97.69 (8), 100.20 (10)		

345

346



347

348

349 Figure 1. Pinkish-brown pauloabibite intergrown with an unidentified Ca-Nb oxide,

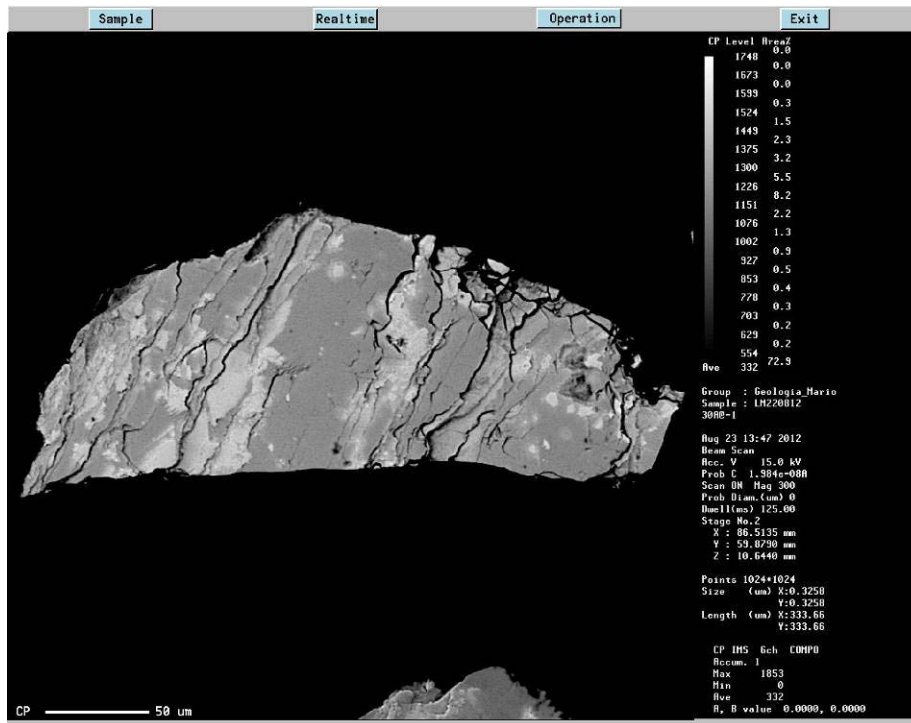
350 with dolomite (white) and tochilinite (black), from the Jacupiranga mine, Cajati,

351 São Paulo, Brazil. Field of view: 4 mm.

352

353

354



355

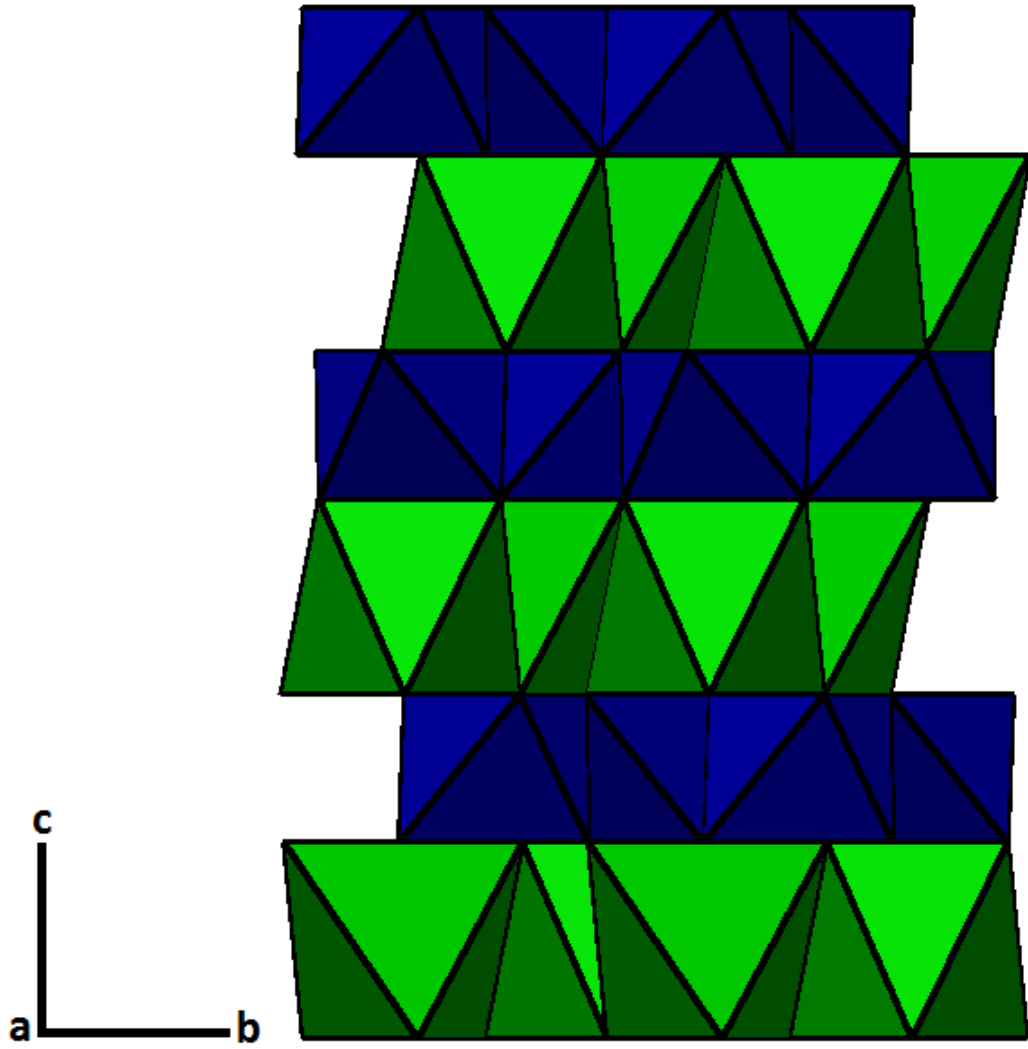
356

357

Figure 2. Back-scattered electron image of pauloabibite (dark) intergrown with an unidentified Ca-Nb oxide (light).

358

359



360  
361  
362  
363  
364

Figure 3. Crystal structure of pauloabibite. NaO<sub>6</sub> octahedra are green and NbO<sub>6</sub> octahedra are blue.



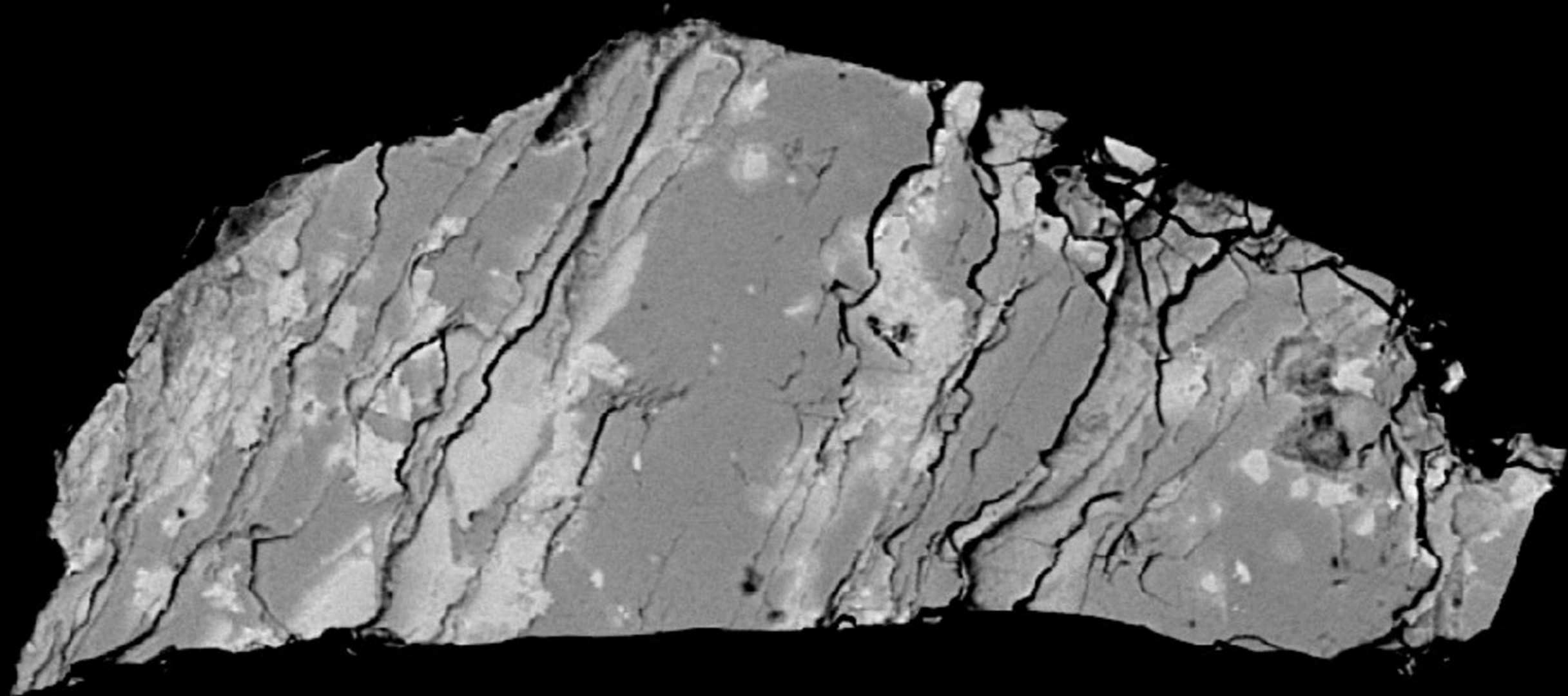


Sample

Realtime

Operation

Exit



CP Level	Area%
1748	0.0
1673	0.0
1599	0.0
1524	0.3
1449	1.5
1375	2.3
1300	3.2
1226	5.5
1151	8.2
1076	2.2
1002	1.3
927	0.9
853	0.5
778	0.4
703	0.3
629	0.2
554	0.2
Ave	332 72.9

Group : Geologia\_Mario  
 Sample : LM220812  
 30AC-1

Aug 23 13:47 2012  
 Beam Scan  
 Acc. V 15.0 kV  
 Prob C 1.984e-08A  
 Scan ON Mag 300  
 Prob Diam.(um) 0  
 Dwell(ms) 125.00  
 Stage No.2  
 X : 86.5135 mm  
 Y : 59.8790 mm  
 Z : 10.6440 mm

Points 1024\*1024  
 Size (um) X:0.3258  
 Y:0.3258  
 Length (um) X:333.66  
 Y:333.66

CP IMS 6ch COMPO  
 Accum. 1  
 Max 1853  
 Min 0  
 Ave 332  
 A, B value 0.0000, 0.0000

CP  50 um

a b c

